Topological Classification of Drainage Networks in the South Island of New Zealand

Yasmin Walley[1*], Alex Henshaw[1], James Brasington[1,2]

[1] Queen Mary, University of London, School of Geography, London, United Kingdom; [2] University of Waikato, Department of Earth and Ocean Sciences, Hamilton, New Zealand

* Corresponding Author: y.r.s.walley@qmul.ac.uk

Queen Mary University of London

INTRODUCTION

The pattern of sediment transfer through the catchment system is modulated by the interaction of key network characteristics, such as the distribution of transport capacity and resultant zones of sediment storage. This research project will investigate the role that network topology plays in this process using a numerical model of sediment production, storage and transfer in the South Island of New Zealand. A method of identifying representative topological structures is presented, in which five network 'types' have been identified from a range of networks.

DATA PREPARATION

59 catchments were identified in the South Island of New Zealand with a minimum catchment area of 300 km^2. The catchments were clipped to the piedmont of the Southern Alps to remove diffusive environments. The river networks were extracted in MATLAB using the method outlined by Tarboton (2013; Fig. 1), which includes identifying a network skeleton of upwardly curved grid cells (Peucker and Douglas, 1975), and calculating a channel head threshold value by drop analysis (Tarboton et al., 1991, 1992).

A numerical connectivity structure was generated, in which four numerical values in each link refer to the ID numbers of the link itself, the two upstream links and the link immediately downstream. Key parameters were also calculated for each network link, including topographic variables (e.g. slope, drainage density), and network magnitude (e.g. Strahler order, Shreve magnitude).

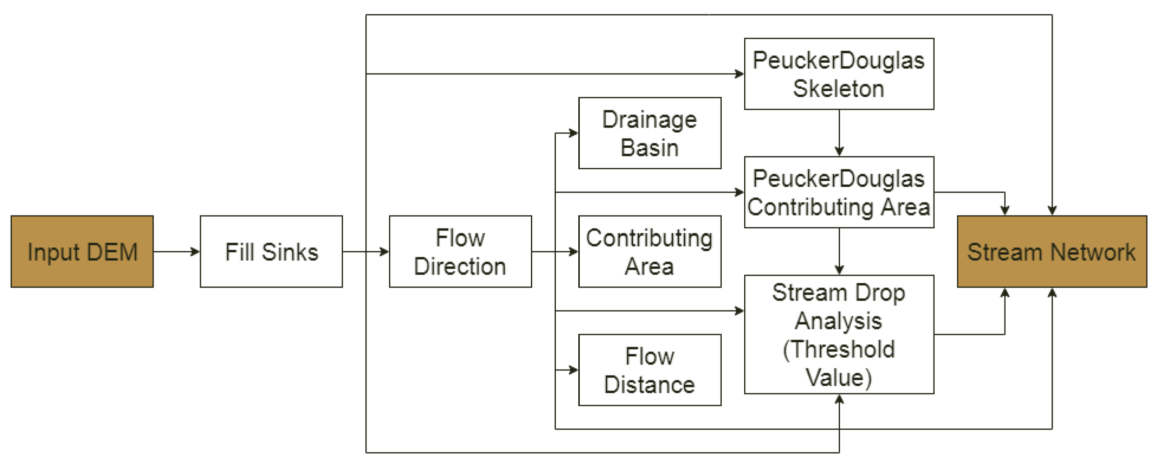

(Fig. 1) The process of network extraction employed in each catchment.

TOPOLOGICAL CLASSIFICATION

Topological variables were identified, which incorporate network magnitude, branching and geometry, as well as catchment size and shape. The values were calculated at the outlet of each network, and six key parameters of network topology were identified to be statistically significant (Table 1). Principal Component Analysis (PCA) derived two significant components representing a combined 53% of the variance, and were interpreted to represent network magnitude (PC1) and topography (PC2).

Agglomerative Hierarchical Clustering (AHC) was performed using the two principal components, using the Euclidean dissimilarity distance measure. Five clusters were identified, with catchment membership consistency across five linkage methods (Fig. 2a). Kruskal-Wallis with Dunn's multiple comparison tests revealed statistically significant differences ($p < 0.0001$) between the resulting clusters.

Final groupings were validated using the *k*-means clustering method as a comparison (Fig. 2b). This method assumes spherical clusters of similar sizes, thus the analysis produced very similar clusters to the AHC method, allowing for the misclassification of data points around the edges of large groups. This similarity is furthered by removing the smallest cluster.

Parameters	Loadings	Description	Source
Strahler Order (Ω)	-0.75 (PC1)	Value at outlet	Strahler (1957)
Network Structure (c)	0.87 (PC1)	Value at outlet	Zanardo et al. (2013) Walley et al. (2018)
Width Ratio	0.55 (PC1)	16/84 ratio of number of links per band*	n/a
Elevation Ratio	0.74 (PC2)	16/84 ratio of mean elevation per band*	n/a
Drainage Density (km/km^2)	-0.63 (PC2)	Value at outlet	n/a
Confluence Angle (°)	0.76 (PC2)	Mean of all confluences	Seybold et al. (2017)

(Table 1) Parameters of network topology.

The ratio between the 16th and 84th percentile was calculated by separating the catchment into 5% bands based on flow distance to the outlet. Values were calculated using the centre of each link.

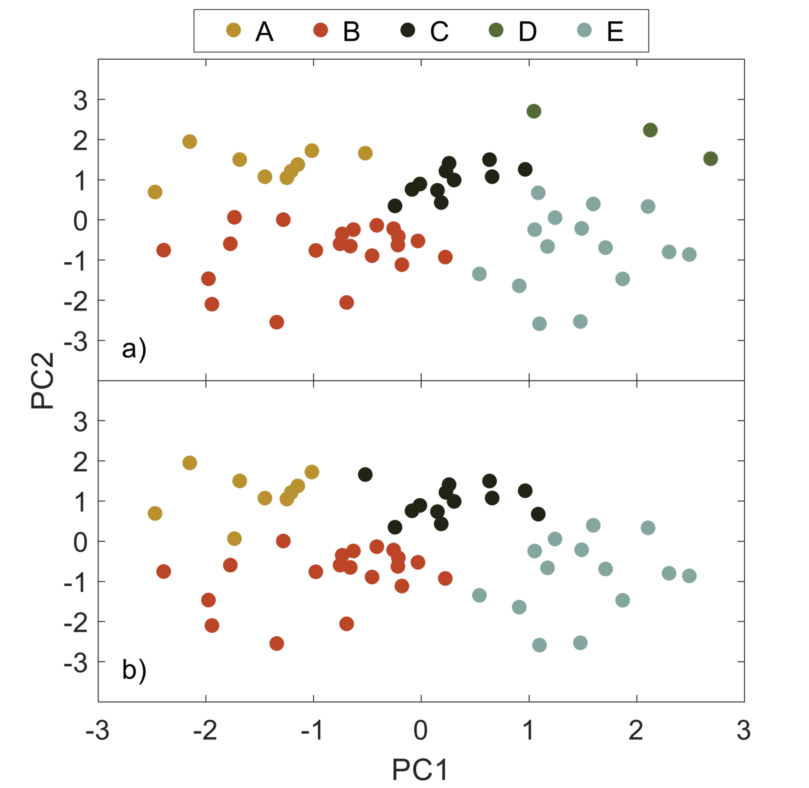

(Fig. 2) Agglomerative Hierarchical Clustering (a) and *k*-means clustering (b) results. The latter shows the clusters produced when the smallest group is excluded.

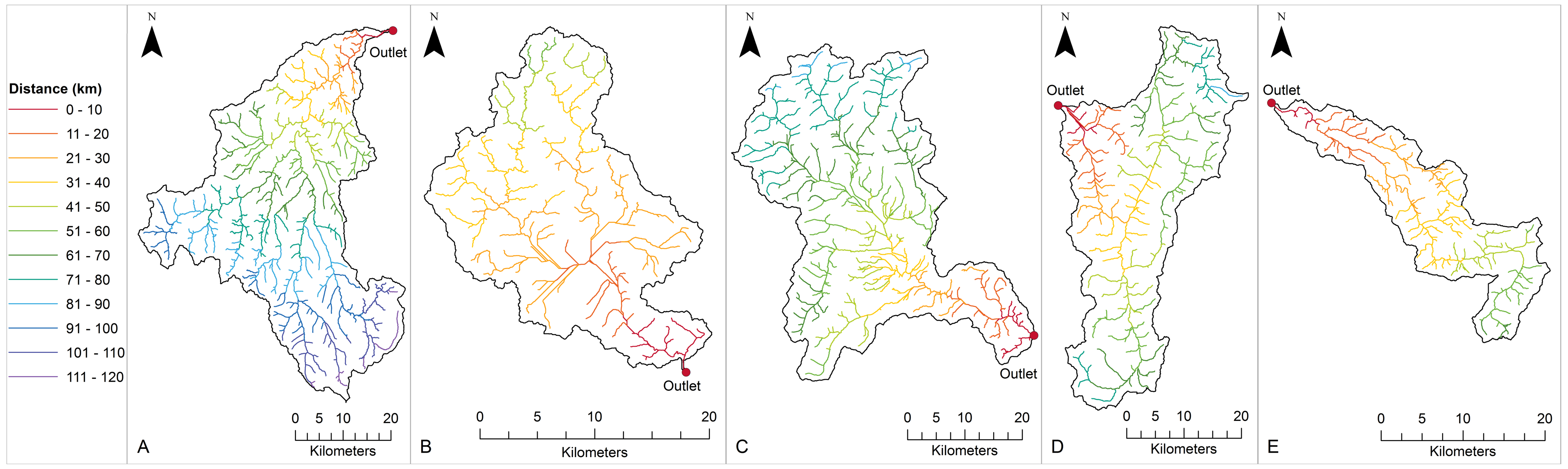

(Fig. 3) The five catchments identified as the central object in each cluster. The flow distance to the outlet is indicated in 10km distance intervals. The Motueka River (A) represents catchments with high Strahler values and large angles at tributary junctions, and the Tokomairiro River (B) represents catchments with high Strahler values and drainage density. The Rangitata River (C) is the largest catchment and represents those with mid-range values, while the Hollyford River (D) represents three outlier catchments with very high tributary angles and *c* values. The Arahura River (E) is the smallest catchment, and represents those with high *c* values and drainage density.

DISCUSSION

The five catchments in Fig. 3 were identified as the objects closest to the centroid of each cluster, and thus representative of the network topologies in that group. The parameter values for each class indicate decreasing size and increasing structural influence (Table 2).

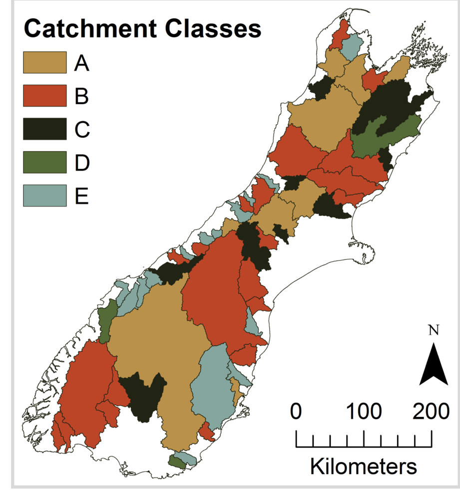

(Fig. 4) Classified map of South Island catchments.

The distribution of classes in Fig. 4 does not reflect the strong climatic divide between the east and west coasts, thus the relationship between mean angle and aridity in Seybold et al. (2017) is not evident. It is possible that the region's significant tectonic activity is overriding topological signals from other sources.

A distinct difference in patterns of sediment connectivity is expected to emerge across the classes, particularly between those of different *c* values (Walley et al., 2018). A numerical model of sediment production, storage and transfer will be used to explore these patterns, and address questions relating to the timescales associated with pulses of co-seismic sediment production.

Class	Strahler Order (Ω) *Median*	Network Structure (c)	Width Ratio	Elevation Ratio	Drainage Density (km/km^2)	Confluence Angle (°) *Mean*
A	6	Low	Wide Centre	Straight-Convex	Mid	72.6
B	5	Low	Consistent Width and Wide Centre	Straight-Concave	High	64.5
C	5	Mid	Wide Headwaters	Straight	Mid	72.0
D	4	High	Consistent Width	Convex	Low	78.3
E	4	High	Consistent Width	Straight-Concave	High	66.1

(Table 2) Parameter values in each class.

REFERENCES

Peucker, T. K., & Douglas, D. H. (1975). Detection of Surface-Specific Points by Local Parallel Processing of Discrete Terrain Elevation Data. *Computer Graphics and Image Processing*, *4*, 375–387.

Seybold, H., Rothman, D. H., & Kirchner, J. W. (2017). Climate's watermark in the geometry of stream networks. *Geophysical Research Letters*, *44*, 2272–2280.

Strahler, A. N. (1957). Quantitative Analysis of Watershed Geomorphology. *EOS, Transations American Geophysical Union*, *38*(6), 913–920.

Tarboton, D. G. (2013). TauDEM 5.1 Guide to using the TauDEM Command Line Functions.

Tarboton, D. G., Bras, R. L., & Rodriguez-Iturbe, I. (1991). On the extraction of channel networks from digital elevation data. *Hydrological Processes*, *5*(1), 81–100.

Tarboton, D. G., Bras, R. L., & Rodriguez-Iturbe, I. (1992). A physical basis for drainage density. *Geomorphology*, *5*(1–2), 59–76.

Walley, Y. R. S., Tunnicliffe, J. F., & Brierley, G. J. (2018). Network structure and sediment routing in two disturbed catchments, East Cape, New Zealand. *Geomorphology*, *307*, 38-49.

Zanardo, S., Zaliapin, I., & Foufoula-Georgiou, E. (2013). Are American rivers Tokunaga self-similar? New results on fluvial network topology and its climatic dependence. *Journal of Geophysical Research: Earth Surface*, *118*, 166–183.